Response of laminated glass elements subject to dynamic loadings using a monolithic model and a stress effective Young's modulus

M. L. Aenlle[1], F. Pelayo[1], A. Alvarez-Vázquez[1], N. García-Fernandez[1], M. Muñiz-Calvente[1]

[1] Department con Construction and Manufacturing Engineering. University of Oviedo. Gijón, Spain.

Corresponding author: F. Pelayo, Email: fernandezpelayo@uniovi.es

Abstract

Due to the brittle nature of the glass, to study the response of glass elements subjected to dynamics loadings is of great interest, mainly when human injury resulting from glass breakage may occur. Laminated glass consists of two or more layers of monolithic glass and one or more viscoelastic interlayers. In this paper, a technique to predict the dynamic response (deflections and stresses) of laminated glass elements using a linear elastic monolithic model is proposed and validated. In a first step, the modal parameters and the dynamic response of a monolithic model are calculated using the modal superposition technique. Then, the modal parameters and the modal coordinates of the laminated glass element are estimated using the equations derived in this paper. Finally, the stresses in time and frequency domain are estimated using an effective stress Young's modulus.

Keywords: *Effective Young's modulus, Stress estimation, Dynamic loadings, Impact test.*

1. Introduction

Laminated glass elements are nowadays used in many structural applications (floor glazing, facades, security glass, blast resistant glass, ballistic resistant glass, etc.). Laminated glass beams and plates consist of two or more layers of monolithic glass and one or more interlayers (usually of a polymeric material), which exhibit a viscoelastic behaviour[1], the mechanical properties being

time and temperature dependent[2,3]. The flexural stiffness provided by the interlayers are usually neglected but they provide shear stresses constraining the relative sliding of the glass plies[4], which contributes to the bending stiffness of laminated glass elements[5].

Laminated glass elements are subject to static and dynamic loadings and they have to be designed under safety conditions. The calculations of these elements are very high time consuming when a dynamic or a static full viscoelastic analysis is performed, because the response is time-dependent and fine meshes are required. The thickness of the interlayers is usually very small compared with the other dimensions of the element, and numerical models must be meshed with many small 3D elements.

In order to simplify the calculations in laminated glass elements, some authors have proposed to consider the polymeric interlayers as linear elastic materials[6–8], neglecting the "memory effect" of viscoelasticity. Another relevant simplification in the static calculations is the concept of effective thickness proposed by Bennisson et al.[6,7], which consists of considering of a monolithic beam with the same bending stiffness as that of the laminated beam. Galuppi and Royer-Carfagni[8] developed a model to calculate the static deflection and the stresses of laminated glass beams composed of two glass layers and one polymeric interlayer. Later, this model was extended to multilayered glass beams and to laminated glass plates[9]. On the other hand, several models were derived to predict the modal parameters of sandwich beams with viscoelastic core[10–14], which have been recently particularized for laminated glass elements[15,16], as well as to estimate stresses in frequency domain[17].

In this paper, a technique to predict the dynamic response (deflection and stresses) of laminated glass elements using a linear elastic monolithic model is proposed. Firstly, the modal parameters (natural frequencies, damping ratios and mode shapes) of the linear elastic monolithic model are

calculated. Secondly, the dynamic response of the monolithic model subject to the dynamic loading is determined using the modal superposition technique[18]. Finally, the modal parameters and the modal coordinates of the laminated glass element are estimated using the equations derived in this paper. Moreover, an effective stress Young's modulus, constant for each mode, has been derived, which can be used for calculating dynamic stresses in both time and frequency domain. The methodology has been validated by numerical simulations and experimental tests subjecting a laminated glass beam to dynamic loadings.

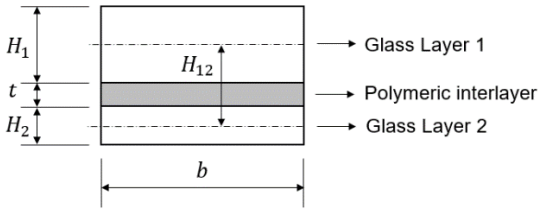

Figure 1. Cross-section of a laminated glass beam

2. Theory

Static and dynamic stiffness

Galuppi and Royer-Carfagni[8] derived an analytical expression for the static deflection of a laminated glass beam composed of two glass layers and one polymeric interlayer, where the stiffness *EI* can be expressed as:

$$EI = EI_T \left(1 + \frac{Y}{1+\frac{EH_1tH_2}{G_t(H_1+H_2)}\psi_B}\right) \quad (1)$$

where E is the Young's modulus of the glass layers, G_t is the shear modulus of the polymeric interlayer, H_1 and H_2 are the thicknesses of the glass layers, t is the thickness of the polymeric interlayer and ψ_B is a parameter dependent on the boundary conditions. The expressions of EI_T (stiffness of the glass layers) and Y (geometric parameter), are shown in the nomenclature.

Equating Eq. (1) to the stiffness of a monolithic model with constant thickness $H_{TOT} = H_1 + t + H_2$, that is,

$$EI = \frac{E_{eff} b H_{TOT}^3}{12} \tag{2}$$

the following expression for the static effective Young's modulus is obtained[16]:

$$E_{eff} = \frac{E}{1+Y}\left(1 + \frac{Y}{1+\frac{EH_1 t H_2}{G_t(H_1+H_2)}}\right) \tag{3}$$

Aenlle and Pelayo[16], based on the model of Ross, Kerwin and Ungar[10,11], derived and expression for the effective complex flexural stiffness of a three-layered beam, which is given by:

$$EI^*(\omega,T) = EI_T\left(1 + \frac{Y}{1+\frac{EH_1 t H_2 k_I^2(\omega,T)}{G_t^*(\omega,T)(H_1+H_2)}}\right) \tag{4}$$

where $G_t^*(\omega,T)$ is the complex shear modulus of the interlayer and $k_I(\omega,T)$ is the wavenumber. From Eq. (4), the following expression for the dynamic effective Young's modulus is derived:

$$E_{eff}^*(\omega,T) = \frac{E}{1+Y}\left(1 + \frac{Y}{1+\frac{EH_1 t H_2 k_I^2(\omega,T)}{G_t^*(\omega,T)(H_1+H_2)}}\right) \tag{5}$$

Stresses in frequency domain

Aenlle et al.[17] derived an expression for estimating stresses in the glass layers of a three-layered laminated glass beam (see Figure 1) in the frequency domain. The stresses at the top of layer 1 can be calculated by means of the expression:

$$\sigma_1(x,\omega,T) = E_{1\sigma eff}(\omega,T)\frac{H_1}{2}w''(x,\omega,T) \tag{6}$$

where $E_{1\sigma eff}(\omega,T)$ is the dynamic stress effective Young's modulus for layer 1, given by:

$$E_{1\sigma eff}(\omega,T) = E\left[\frac{1}{Y}\left(\frac{EI^*(\omega,T)}{EI_T} - 1\right)\frac{H_2 H_{12}}{H_1+H_2}\frac{2}{H_2} + 1\right] \tag{7}$$

where H_{12} is the distance between the medium planes of glass layers (see nomenclature). On the other hand, the stresses at the bottom of layer 2 can be obtained by means of the equation:

$$\sigma_2(x,\omega,T) = E_{2\sigma eff}(\omega,T)\frac{H_2}{2}w''(x,\omega,T) \quad (8)$$

where $E_{2\sigma eff}(\omega,T)$ is the dynamic stress effective Young's modulus for layer 2, that is,

$$E_{2\sigma eff}(\omega,T) = E\left[\frac{1}{Y}\left(\frac{EI^*(\omega,T)}{EI_T}-1\right)\frac{H_1H_{12}}{H_1+H_2}\frac{2}{H_2}+1\right] \quad (9)$$

If $H_1 = H_2$, then $E_{1\sigma eff}(\omega,T) = E_{2\sigma eff}(\omega,T)$

3. Using monolithic models

The modal parameters of a laminated glass beam can be determined using a monolithic model of constant thickness H_{TOT} and a frequency and temperature dependent effective Young's modulus $E^*_{eff}(\omega,T)$[15]. Although this effective Young's modulus can be used in analytical equations, this mechanical behavior is difficult to reproduce in a finite element program because it cannot be modelled as a viscoelastic material, the reason being that the effective Young's modulus $E^*_{eff}(\omega,T)$cannot be estimated as the Fourier transform of the static effective Young's modulus $E_{eff}(t,T)$. A way to overcome this drawback consists of assembling a linear-elastic monolithic model with constant stiffness$EI_{\text{mon}} = (EbH^3_{\text{TOT}})/12$ and masss per unit length $m_{\text{mon}} = \rho_{\text{mon}}H_{\text{TOT}}$, from which the natural frequencies ω_{mon} and mass normalized mode shapes ϕ_{mon} can be calculated.

From the equation of motion of a continuous system[18] without damping or with proportional damping, the following expression to calculate the natural frequencies of a linear-elastic monolithic beam is derived:

$$\omega^2_{mon} = k_I^4\frac{EI_{mon}}{m_{mon}} \quad (10)$$

where the wavenumber k_I is constant for each mode. On the other hand, the natural frequencies and loss factors of a laminated glass beam with the same geometry and boundary conditions can be obtained by[15,16]:

$$\omega^2(1+j\eta) = (k_R + jk_I)^4 \frac{E^*_{eff}(\omega,T)H^3_{TOT}}{12\rho b H_{TOT}} \quad (11)$$

where ρ is the apparent mass density of the laminated glass beam and η the loss factor.

If we assume that wavenumbers k_I for both the monolithic and the laminated glass beams are equal, and k_I is isolated in Eq. (10) and substituted in Eq. (11), the later results in:

$$\omega^2(1+j\eta) = \left(k_R + j\left(\frac{\omega^2_{mon} m_{mon}}{EI_{mon}}\right)^{1/4}\right)^4 \frac{E^*_{eff}(\omega,T)H^3_{TOT}}{12\rho b H_{TOT}} \quad (12)$$

Values for k_R are not tabulated in the literature and no simple equations to calculate this parameter have been proposed. They can be obtained solving the 6th order differential equation developed by Mead and Markus[13], but the calculations are not easy and must be programmed for each boundary condition. Assuming k_R = 0 in Eq. (12) it simplifies to:

$$\omega^2(1+j\eta) = \omega_{mon} \frac{\rho_{mon}}{\rho} \frac{E_{eff}(\omega,T)}{E} \quad (13)$$

With respect to the mode shapes, it has been experimentally demonstrated by the authors[19] that there are not discrepancies between the mode shapes of a monolithic and a laminated glass beam with the same geometry and boundary conditions, i.e., it can be assumed that:

$$\psi_{mon} \cong \psi \quad (14)$$

where ψ_{mon} and ψ are the unscaled mode shapes of the monolithic and the laminated models, respectively. However, due to the fact that the mass of each beam (monolithic and laminated) is different, the mass normalized mode shapes are related by:

$$\phi_{mon}\sqrt{m_{mon}} \cong \phi\sqrt{m} \quad (15)$$

where m is the modal mass of the laminated beam. Moreover, the modal masses are related by:

$$m = m_{mon}\frac{\rho}{\rho_{mon}} \tag{16}$$

and Eq. (15) can be rewritten as:

$$\phi \cong \phi_{mon}\sqrt{\frac{\rho_{mon}}{\rho}} \tag{17}$$

4. Displacements and stresses in frequency-domain

The response of a laminated glass beam can be expressed in terms of mode shapes by[18]:

$$w(x,\omega,T) = \sum_{i=1}^{N_{modes}} \phi_i(x) q_i(\omega,T) \tag{18}$$

where $\phi_i(x)$nd $q_i(\omega,T)$ are the *i*-th mode shape and the *i*-th modal coordinate, respectively. If Eq. (18) is substituted in Eqs. (6) and (7), the stresses in frequency-domain can be estimated by:

$$\sigma_1(x,\omega,T) = E_{1\sigma eff}(\omega,T)\frac{H_1}{2}\sum_{i=1}^{N_{modes}} \phi_i''(x) q_i(\omega,T) \tag{19}$$

$$\sigma_2(x,\omega,T) = E_{2\sigma eff}(\omega,T)\frac{H_2}{2}\sum_{i=1}^{N_{modes}} \phi_i''(x) q_i(\omega,T) \tag{20}$$

where $\phi_i''(x)$ indicates strain mode shape (second derivative of the mode shape). The mode shape $\phi_i(x)$ needed in Eqs. (18-20) can be obtained from a linear elastic monolithic model by means of Eq. (17). With respect to the frequency-domain modal coordinates, they can be estimated by[18]:

$$q_i(\omega,T) = \frac{\int_0^L \phi_i(x) p(x,\omega) dx}{m_i\left(\omega_i^2(T) - \omega^2 + j\eta_i(T)\omega_i^2(T)\right)} \tag{21}$$

where ω_i,η_i and m_i are the natural frequency, loss factor and modal mass of the *i*-th mode, respectively, and $p(x,\omega)$ is the force exciting the system.

The modal parameters ω_i and η_i needed in Eq. (21) can be obtained with two different techniques:

1. To use a monolithic model (analytical or numerical) and calculate the modal parameters ω_i and η_i with Eq. (13) and the modal masses m_i with Eq. (16). With respect to the mode shapes ψ_i of the laminated glass beam, they can be considered equal to those of the monolithic model[15-17].

2. To use the experimental modal parameters of the laminated glass beam estimated with modal analysis.

Eq. (21) can be avoided if the experimental modal parameters and the experimental responses $w(x,\omega,T)$ of the beam are known, because the experimental modal coordinates can be estimated from Eq. (18).

If a discrete model is used, Eq. (21) becomes:

$$q_i(\omega,T) = \frac{\phi_i^T p(\omega)}{m_i\left(\omega_i^2(T)-\omega^2+j\eta_i(T)\omega_i^2(T)\right)} \tag{22}$$

An alternative to Eq. (22) consists of using the dynamic response of a monolithic model with the same geometry and boundary conditions. The modal coordinates $q_{imon}(\omega,T)$ of a linear elastic monolithic model subject to the same force $p(x,\omega)$, can be obtained from the equations:

$$q_{i_{mon}}(\omega,T) = \frac{\int_0^L \phi_{i_{mon}}(x)p(x,\omega)dx}{m_{i_{mon}}\left(\omega_{i\ mon}^2-\omega^2+j2\omega\xi_{i_{mon}}\omega_{i_{mon}}\right)} \tag{23}$$

If equal mode shapes are assumed for both the laminated and the monolithic beam[19], the following equation is fulfilled:

$$\int_0^L \psi_i(x)p(x,\omega)dx = \int_0^L \psi_{i_{mon}}(x)p(x,\omega)dx \tag{24}$$

from which the following relationship between the modal coordinates $q_i(\omega,T)$ and $q_{imon}(\omega,T)$ is derived:

$$q_i(\omega,T) = q_{i_{mon}}(\omega)\frac{m_{i_{mon}}^{3/2}\left(\omega_{i\ mon}^2-\omega^2+j2\omega\xi_{i_{mon}}\omega_{i_{mon}}\right)}{m_i^{3/2}\left(\omega_i^2(T)-\omega^2+j\eta_i(T)\omega_i(T)^2\right)} \tag{25}$$

If Eq. (25) is substituted in Eqs. (19) and (20), the stresses in the glass layers of a laminated glass beam can be estimated using the response of a monolithic model.

An important simplification can be made in Eqs. (19) and (20) if the effective Young's modulus $E_{1\sigma eff}(\omega, T)$ and $E_{2\sigma eff}(\omega, T)$are constant for each mode. In this paper, it is proposed to consider for the *i*-th mode the effective Young's modulus given by:

$$E_{1\sigma_i}(T) = E_{1\sigma_{eff}}(\omega_i, T) \tag{26}$$

$$E_{2\sigma_i}(T) = E_{2\sigma_{eff}}(\omega_i, T) \tag{27}$$

Since the effective Young's modulus $E_{1\sigma i}(T)$ and $E_{2\sigma i}(T)$ are not frequency dependent, they can be used in both time and frequency domain, i.e., they can be considered stress effective Young's modulus for layers 1 and 2, respectively, for both time and frequency domains.

5. Stresses in time-domain

With the assumptions considered in Eqs. (26) and (27), the stresses in the frequency domain at the top of layer 1, and at the bottom of layer 2, can be obtained with the expressions:

$$\sigma_1(x, \omega, T) \cong \frac{H_1}{2} \sum_{i=1}^{N_{modes}} E_{1\sigma i}(T) \phi_i''(x) q_i(\omega, T) \tag{28}$$

$$\sigma_2(x, \omega, T) \cong \frac{H_2}{2} \sum_{i=1}^{N_{modes}} E_{2\sigma i}(T) \phi_i''(x) q_i(\omega, T) \tag{29}$$

Due to the fact that $E_{1\sigma i}(T)$ and $E_{2\sigma i}(T)$ are not time-dependent, the stresses in time-domain can be estimated by modal superposition avoiding the convolution of the responses.

On the other hand, if the inverse Fourier transform is applied to Eqs. (28) and (29), they become:

$$\sigma_1(x, t, T) \cong \frac{H_1}{2} \sum_{i=1}^{N_{modes}} E_{1\sigma i}(T) \phi_i''(x) q_i(t, T) \tag{30}$$

$$\sigma_2(x, t, T) \cong \frac{H_2}{2} \sum_{i=1}^{N_{modes}} E_{2\sigma i}(T) \phi_i''(x) q_i(t, T) \tag{31}$$

The time domain modal coordinates $q_i(t, T)$ can be retrieved by inverse Fourier transformation of Eq. (25).

6. Validation of the methodology: numerical model

In order to validate the technique proposed in this paper, the modal parameters and the displacement and stress responses of a simply supported laminated glass beam, made of annealed glass layers, PVB core and with the following geometrical data: L = 1 m, H_1 = 4 mm, t = 0.76 mm, H_2 = 4 mm, b = 0.1 m, were predicted at different temperatures using Eqs.(30) to (31), and validated with a numerical model assembled in ABAQUS[22].

Finite element models

Two Finite Element (FE) models were assembled:

- A simply supported monolithic glass model with thickness $H_{TOT} = H_1 + t + H_2 = 8.76\,mm$. The mechanical properties presented in Table 1 were considered in the simulations. The beam was meshed using quadratic hexahedral elements (20 nodes per element) with an approximate size of 4 mm. The model is shown in Figure 2.
- A layered model (see Figure 2) with glass layers modelled as linear elastic and the PVB interlayer model as linear viscoelastic[23, 24], was also meshed using 3 quadratic hexahedral elements through the beam thickness (one element for each material layer). The mechanical properties presented in Table 1, together with the parameters of the Prony series presented in Table A1, were considered in the simulations. The effect of temperature in the PVB was considered by means of the Williams-Landel-Ferry (WLF) equation[25] using constants C_1 and C_2.

The natural frequencies ω_{mon}, mode shapes ψ_{mon} and modal masses m_{mon}, corresponding to the first four bending modes of the monolithic model, were obtained solving the eigenvalue problem, and the results are presented in Tables 2, 3 and 4, for the temperatures of 20, 25 and 30^{o}C, respectively. The wavenumbers k_I were estimated from the monolithic model using eq. (10).

Table 1. Mechanical properties of glass and PVB[24] (E: Young's Modulus, v: Poisson's ratio, ρ: density, G_0: instantaneous shear modulus, K: bulk modulus, C_1 and C_2: Williams-Landel-Ferry constants at $T_{ref} = 20^o$ C).

Glass			PVB					
E	v	ρ	G_0	K	v	ρ	C_1	C_2
[GPa]	[-]	[kg/m^3]	[GPa]	[GPa]	[-]	[kg/m^3]	[-]	[-]
70	0.22	2500	0.3696	2	0.40	1046	12.60	74.46

With respect to the layered model, a steady-state dynamic analysis (linear perturbation procedure) in the frequency domain was carried out, exciting the beam with two harmonic concentrated loads (see Figure 2) in the frequency range 0-400 Hz (frequency sweep).

The natural frequencies and the corresponding loss factors were estimated from the frequency response function (FRF), which was isolated around the peaks of resonance and taken to the time domain using the Inverse Discrete Fourier Transform (IDFT). The resonance frequency is obtained by determining the zero crossing times, and the damping by the logarithmic decrement of the corresponding free decay. The predicted natural frequencies and loss factors at 20, 25 and 30ºC are shown in Tables 2, 3 and 4, respectively.

The modal parameters of the laminated glass beam were also estimated using Eqs. (13) and (16). From Tables 2, 3 and 4 it is concluded that the modal parameters have been predicted with a good accuracy. Although damping estimation in laminated glass panels using Eq. (13) are not accurate, in this particular case (simply supported beam) $k_R = 0$ for all the modes (which is the assumption considered for deriving Eq. (14)), which explains the large precision of the predictions.

Table 2. Modal parameters at 20º C.

Mode	Monolithic glass beam		Laminated glass beam					
	Nat. freq	Modal mass	Nat. freq [Hz]		Loss factor		Modal mass [kg]	
	[Hz]	[kg]	Eq. (14)	FEM Visco	Eq. (14)	FEM Visco	Eq. (17)	FEM
1	21.31	1.091	21.71	21.718	0.0069	0.0070	1.0365	1.036
2	85.24	1.081	85.91	86.00	0.0157	0.0162	1.0270	1.0265
3	191.72	1.065	190.27	190.40	0.0219	0.0220	1.0117	1.0133
4	340.48	1.047	331.60	330.20	0.0309	0.03182	0.9947	1.0004

Table 3. Modal parameters at 25º C.

Mode	Monolithic glass beam		Laminated glass beam					
	Nat. freq	Modal mass	Nat. freq [Hz]		Loss factor		Modal mass [kg]	
	[Hz]	[kg]	Eq. (14)	FEM Visco	Eq. (14)	FEM Visco	Eq. (17)	FEM
1	21.31	1.091	21.60	21.62	0.0154	0.0157	1.0365	1.036
2	85.24	1.081	85.86	84.95	0.0305	0.0306	1.0270	1.0265
3	191.72	1.065	186.49	186.81	0.0497	0.0488	1.0117	1.0133
4	340.48	1.047	323.81	324.50	0.0683	0.0715	0.9947	1.0004

The stresses at point A (mid-point of the beam) and at point B (see Figure 2) estimated with Eqs. (28) and (29) at different temperatures T = 20 ,25 and 30ºC are presented in Figure 3. From the results shown in Figure 3, it can be observed that the stresses have been predicted with a good accuracy (see Table 5) using Eqs. (28) and (29), the error being less than 8 %, which demonstrates that the methodology proposed in this paper can be used to predict accurately the stresses in laminated glass beams.

Table 4. Modal parameters at 30º C.

Mode	Monolithic glass beam		Laminated glass beam					
	Nat. freq	Modal mass	Nat. freq [Hz]		Loss factor		Modal mass [kg]	
	[Hz]	[kg]	Eq. (14)	FEM Visco	Eq. (14)	FEM Visco	Eq. (17)	FEM
1	21.31	1.091	21.44	21.46	0.0356	0.0363	1.0365	1.036
2	85.24	1.081	85.09	83.48	0.0606	0.0612	1.0270	1.0265
3	191.72	1.065	180.92	182.25	0.0907	0.0923	1.0117	1.0133
4	340.48	1.047	310.53	315.40	0.1095	0.1173	0.9947	1.0004

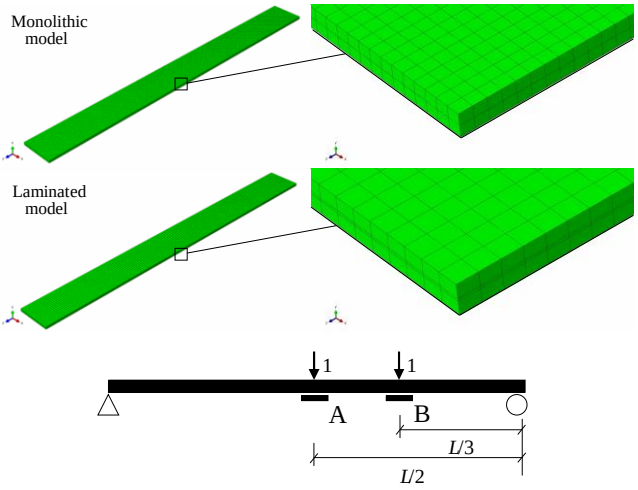

Figure 2. Mesh of the finite element models considered in the simulations for both cases: monolithic and laminated, and harmonic loadings used in the simulations.

7. Validation of the methodology: experimental model

In order to validate by experiments the methodology proposed in this work, the stresses of a laminated glass beam with the following geometrical data: L = 1 m, H_1 = 3 mm, t = 0.38 mm, H_2 = 3 mm, b = 0.1 m, were predicted using Eqs. (30) to (31) and compared with those measured with

two strain gages. The beam, in simply-supported boundary conditions (distance between supports of 0.85 m) was tested at temperatures of 19 and 28° C, respectively, as shown in Figure 4.

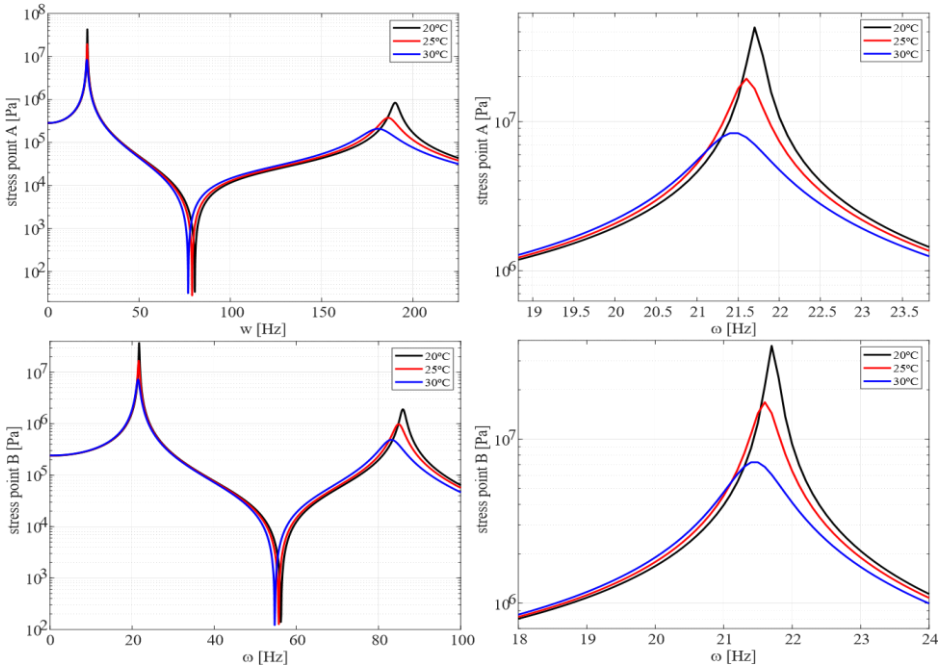

Figure 3. Magnitude of the stresses estimated at the bottom of layer 2 in points A (above) and B (below) for different temperatures (left) and zoomed region for the first mode (right).

Table 5. Stresses obtained with the analytical and the numerical models.

Point	T [° C]	Mode	Numerical model [Pa]	Analytical Eqs. (32) and (33) [Pa]	Error [%]
A	25	1	1.85×10^7	1.94×10^7	4.64
		3	3.72×10^5	3.75×10^5	0.80
	30	1	8.5×10^6	8.4×10^6	1.19
		3	2.05×10^5	2.1×10^5	2.38
B	25	1	1.685×10^7	1.68×10^7	0.298
		2	1.01×10^6	9.81×10^5	2.96
	30	1	7.34×10^6	7.25×10^6	1.24
		2	5.3×10^5	4.9×10^5	8.16

Operational modal analysis

Operational Modal Analysis (OMA) was used to estimate the modal parameters[20]. Small hits applied with an impact hammer, random in time and space, were utilized to excite the beam. The experimental responses were measured with seven uniformly distributed accelerometers (sensitivity of 100 mV/g), the test setup being shown in Figure 4. The responses were recorded for approximately 3 minutes, using a sampling frequency of 2132 Hz. The spectral densities were calculated using 1024 frequency lines and an overlap of 70%. The modal parameters were estimated with the Frequency Domain Decomposition (FDD) technique[20]. In order to reduce the effect of leakage, a proper order of decimation was considered for each mode. The estimated natural frequencies and loss factors are shown in Table 6. The modal analysis provides the damping ratios for each mode, and it has been assumed that $\eta = 2\zeta$, where ζ is the damping ratio.

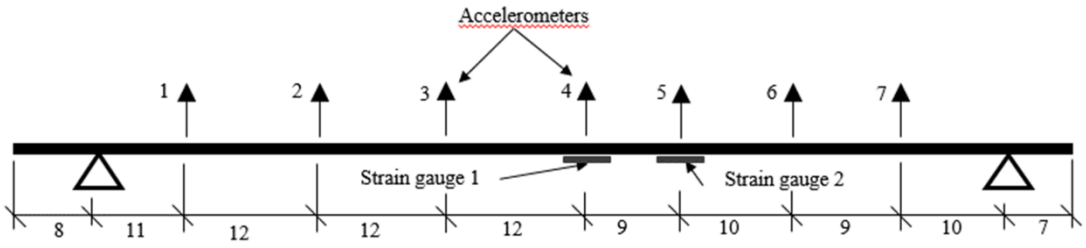

Figure 4. Test setup used in the experiments.

Table 6. Experimental modal parameters for the simply-supported laminated glass beam.

Mode	Temperature 19º C		Temperature 28º C	
	Frequency [Hz]	Loss factor [%]	Frequency [Hz]	Loss factor [%]
1	30.16	4.28	29.00	6.04
2	92.70	1.73	88.93	3.19
3	186.50	2.35	182.14	3.98
4	313.42	2.76	303.92	4.15
5	465.53	2.89	450.34	4.65

Monolithic model

A monolithic finite element model with the same geometry and boundary conditions as the experimental one was assembled in ABAQUS[22].The beam was meshed with 7960 quadratic hexahedral elements C3D20R and the material was modelled as linear-elastic. In order to take into account the effect the rubbery at the supports, the finite element model was updated[25] to achieve a good correlation in natural frequencies and mode shapes. The numerical natural frequencies and mode shapes were obtained by solving the standard eigenvalue problem.

In this paper, the experimental mode shapes were expanded to the un-measured DOF's using the mode shapes of the finite monolithic element model. According to the structural dynamic modification theory[26], the experimental mode shapes can be expressed as a linear combination of the numerical mode shapes[27,28], i.e.:

$$[\phi_x] = [\phi_{FE}][T] \tag{32}$$

where subscripts 'x' and 'FE' indicate experimental and numerical mode shapes, respectively, and $[T]$ is a transformation matrix estimated using the active DOF's, i.e.:

$$[T] = [\phi_{FE}^a][\phi_{ex}^a] \tag{33}$$

where the superscripts *a* indicates active or measured DOF's. Finally, the expanded experimental mode shapes can be estimated with Eq. (32).

Impact tests

The accuracy of the methodology presented in this paper was studied predicting the stresses in the same laminated glass beam when it is subjected to impact loadings. The same test setup (distribution and number of sensors, recording time, sampling frequency, etc.), as that used in the OMA tests, were used to measure the experimental response of the structure. Moreover, two strain

gages HBM LY11-350 were attached at points 1 (not located just in the middle of the span) and 2 (see Figure 4), in order to measure the experimental strains.

The experimental acceleration modal coordinates were estimated with the expression:

$$\{q_x(t,T)\} = [\phi_x(x)]^{+}\{w_x(t,T)\} \quad (34)$$

where the superscript $^{+}$ indicates pseudo-inverse. Then, the experimental displacement modal coordinates were obtained by double integration in the frequency domain.

Due to the fact that the experimental modal coordinates are estimated from the experimental responses, they were used in Eqs. (30) and (31), avoiding the use of Eq. (25).

Stress estimation

The stresses at points 1 and 2 of layer 2 (see Figure 4) were estimated in frequency domain using Eqs. (19) and (20), and in time domain using Eqs. 30) and 31). The mechanical properties shown in Table 1 were used in the calculations. The constant effective Young's modulus, $E_{1\sigma}(T) = E_{2\sigma}(T)$, obtained with Eqs. (26) and (27), are shown in Table 7 for the different tested temperatures.

Table 7. Effective Young's modulus $E_{1\sigma i}(T)$ used in time-domain the calculations.

Mode	Effective Young's Modulus $E_{1\sigma_i} \times 10^{11}$ [GPa]	
	T = 19º C	T = 28º C
1	152.3	151.0
2	151.3	148.8
3	149.9	146.3
4	148.2	143.2
5	146.5	140.1

Discussion

The experimental stresses (time history and spectral density) measured with the strain gauge located at the midpoint of the beam (point 1 in Figure 4) and those predicted with Eqs. (19) and

(20) at 19 and 28º C, respectively, are presented in Figure 5. A small peak (83 Hz) can be observed to the left of the second mode peak, which corresponds to one of the steel frame modes. The stresses were firstly calculated in frequency domain with Eqs. (19) and (20) and the inverse Fourier transform[28] was utilized to obtain the solution in time domain. Since the strain gauge is not located just in the middle of the span, all the modes contribute to the stress. This fact is in agreement with the stresses recorded with the strain gauge (see Figure 5).

The errors between the estimated and the experimental stress power spectral densities at the first natural frequency are presented in Table 8.

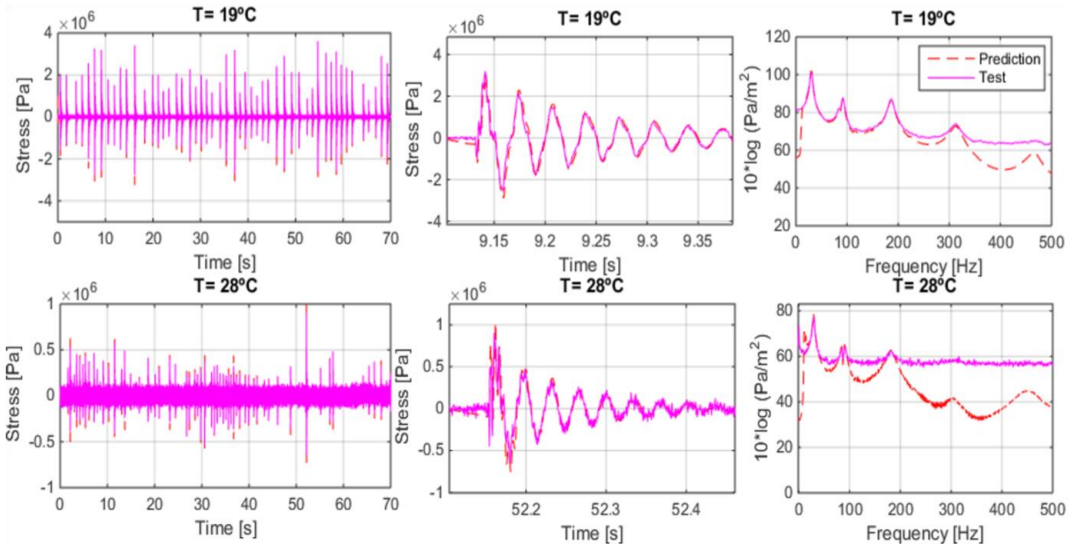

Figure 5. Predicted Eq. (19) and experimental stresses at 19 and 28ºC in point 1: time histories (left), detail of the time histories (center) and power spectral densities (right).

With respect to the contribution of each mode to the total stress (see Figure 7), the first mode is the one which contributes the most, whereas the contribution of the higher modes decreases with increasing temperature. The stresses obtained mode by mode are very similar for the time domain and frequency domain calculations, which demonstrates that the discrepancies between both techniques are small. Thus ,the concept of constant stress effective Young's modulus $E_{i\sigma\text{eff}}(T)$ can

be used to predict with a reasonable accuracy the stresses in laminated glass elements in both time and frequency domain.

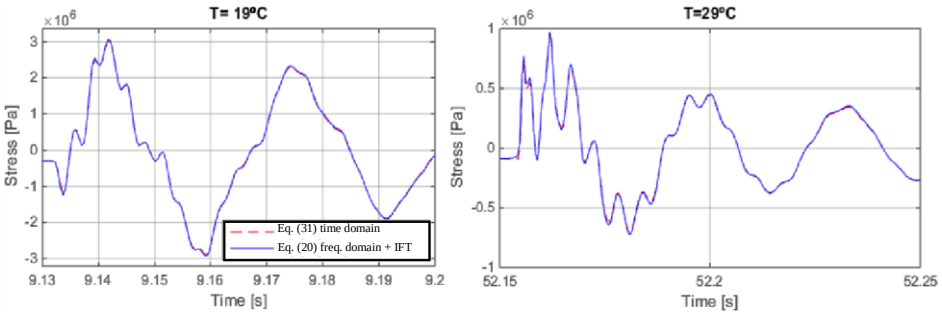

Figure 6. Estimated stresses at point 1 at 19 and 28º C in time domain (Eqs. (30) and (31)) and in frequency domain (Eqs. (19) and (20)) + Inverse Fourier Transform (IFT).

Table 8. Errors at points 1 and 2 between the predicted and the experimental stress spectral densities for the first mode.

Frequency [Hz]	Temperature [º C]	Error [%]	
		Point 1	Point 2
30.16	19	6.26	7.82
29.00	28	8.80	9.11

8. Conclusions

- In this paper, a methodology to predict the dynamic response of laminated glass elements using a linear-elastic monolithic model, has been proposed and validated. The methodology can be applied in both frequency and time domains.
- The methodology was firstly validated comparing the stresses estimated on a simply supported laminated glass using the analytical model proposed in this paper, and those obtained from a numerical model assembled in ABAQUS. The errors between the two models are less than

8%, which demonstrates that the technique can be used to predict with a good accuracy the dynamic response of laminated glass elements.

– The methodology was also validated by experimental tests carried out on a laminated glass beam simply supported in a steel testing frame at 19 and 28º C. The stresses were estimated in time domain being the discrepancies between the experimental and the predicted values less than 8% at 19º C and less that 10% at 28º C for the first mode.

– The stiffness of laminated glass beams decreases with increasing temperature whereas the damping increases. The global effect is that the magnitude of the stresses decreases with increasing temperature.

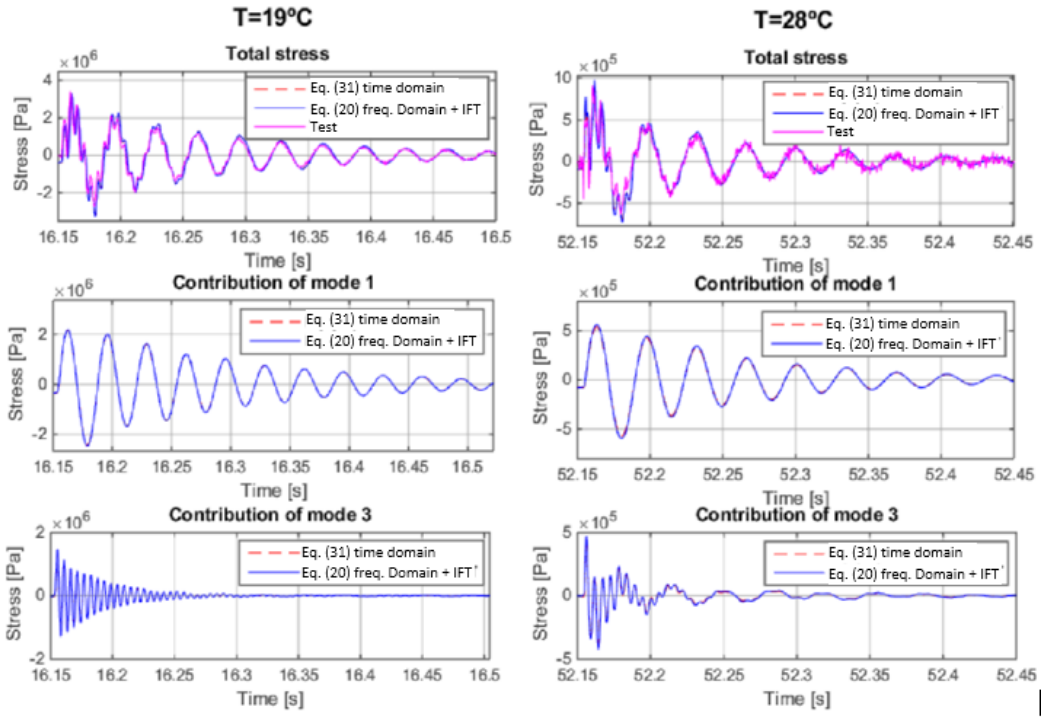

Figure 7. Contribution of the different modes to the total stress at 19 and 28º C in time domain (Eqs. (30) and (31)) and in frequency domain (Eqs. (19) and (20)) + Inverse Fourier Transform (IFT) in point 1.

Declaration of conflicting interests

The authors declare no conflict of interest.

Acknowledgements

The financial support given by the Spanish Ministry of Education through the projects BIA201453774-R and MCI-20-PID2019-105593GB-I00/AEI/10.13039/501100011033 are gratefully appreciated.

References

1. Ferry, J. D. *Viscoelastic Properties of Polymers*. John Wiley & Sons, New York: 1980.
2. Galuppi, L.; Royer-Carfagni, G. F. Laminated beams with viscoelastic interlayer. *Int J Solids Struct*, 49(18):2637–2645, 2012.
3. Lakes, R. S. *Viscoelastic Materials*. Cambridge: Cambridge University Press. 2009.
4. Behr, R. A.; Minor, J. E.; Norvile H. S. Structural behavior of architectural laminated glass. *J Struct Eng*, 119.1:202–222, 1993.
5. Norville, H. S.; King, K. W.; Swoord, J. L. Behaviour and strength of laminated glass. *J Eng Mech*, 124(1):46–53, 1998.
6. Bennison, S.; Qin, M. H. X.; Davies, P. S. High-performance laminated glass for structurally efficient glazing. Innovative Light-weight Structures and Sustainable Facades. innovative Light-Weight Structures and Sustanaible Facades, Hong Kong, 2008.
7. Calderone, I.; Davies, P.S.; and Benninson, S.J. Effective laminate thickness for the design of laminated glass. In *Glass Processing Days*, Tampere, Finland, 2009.
8. Galuppi, L.; Royer-Carfagni, G. F. Effective thickness of laminated glass beams: new expression via a variational approach. *J Struct Eng*, 38:53–67, 2012.

9. Galuppi, L.; Manara, G.; Royer-Carfagni, G. F. Practical expressions for the design of laminated glass. *Compos Part B-Eng*, 45:1677–1688, 2013.
10. Ross, D.; Ungar, E.E.; and Kerwin, E.M. Damping of plate flexural vibrations by means of viscoelastic laminate, Structural Damping, ASME, 49-88, 1959.
11. Ungar, Eric E.; Ross, D.; Kerwin, J. R. Damping of flexural vibrations by alternate viscoelastic and elastic layers. No. AFCRL-TR-60-189. Bolt Beranek and Newman Inc Cambridge MA, 1959.
12. DiTaranto, R.A., and McGraw, Jr, J.R., Vibratory Bending of Damped Laminated Plates. *J Eng Ind*, 91(4):1081–1090, 1969.
13. Mead, D. J.; Markus, S. The forced vibration of a three-layer, damped sandwich beam with arbitrary boundary conditions. *J Sound Vib*, 10(2):163–175, 1969.
14. Asik, M. Z.; Dural, E. Effect of support conditions on the vibration of laminated composite beams. *J Vib Control*, 13:1361–1368, 2017.
15. Lopez-Aenlle, M., Pelayo, F., Frequency Response of Laminated Glass Elements: Analytical´ Modelling and Effective Thickness. *Appl Mech Rev*, 65(2):020802, 2013.
16. Lopez-Aenlle, M.; Pelayo, F. Dynamic effective thickness in laminated-glass beams and´ plates. *Compos Part B-Eng*, 67:332–347, 2014.
17. Aenlle, M. L.; Pelayo, F.; Ismael, G. An effective thickness to estimate stresses in laminated glass beams under dynamic loadings. *Compos Part B-Eng* 82:1–12, 2015.
18. Clough Ray, W.; Penzien, J. *Dynamics of Structures*. Computers & Structures, Inc, 1995.
19. Blasón, S.; López-Aenlle, M.; Pelayo, F. Influence of temperature on the modal parameters of´ laminated glass beams. In *Proc. of the 11th International Conference on Vibration Problems* (ICOVP), Lisbon, Portugal, 2013.

20. Brincker, R.; Ventura, C. *Introduction to Operational Modal Analysis*. John Wiley & Sons, 2015.
21. Nashif, A.D.; Jones, D.I.G.; Henderson, J.P. *Vibration Damping*. John Willey & Sons, New York. 1985.
22. Abaqus User's Manual, Dassault Systemes Simulia Corp., Providence, Rhode Island, USA, 2020.
23. Froling, M.; Persson, K. Computational methods for laminated glass. *J Eng Mech*, 139(7):780– 790, 2013.
24. Pelayo, F., M.J. Lamela-Rey, M. Muniz-Calvente, M. López-Aenlle, A. Álvarez-Vázquez, A. Fernández-Canteli. Study of the time-temperature-dependent behaviour of the PVB: Application to laminated glass elements. Thin-Walled Structures. 119:324-331, 2017
25. Williams, M.L.; Landel, R. F.; Ferry, J. The temperature dependence of relaxation mechanisms in amorphous polymers and other glass-forming liquids. *J Amer Chem Soc*, 77(14):3701–3707, 1955.
26. Sestieri, Structural dynamic modification, *SādhanSā* 25(3):247–259, 2000.
27. Friswell, M.I.; Mottershead, J.E. *Finite Element Model Updating in Structural Dynamics*. Kluwer Academic Publishers, 1995.
28. Brincker, R.; Skafte, A.; Lopez-Aenlle, M.; Sestieri, S.; D'Ambrogio, W.; Canteli, A. A local correspondence principle for mode shapes in structural dynamics, *Mech Syst Signal Pr*, 1(3):91–104, 2014.
29. Tolstov, G. P.; Silverman, R. A. *Fourier Series*. Dover Books on Mathematics. Dover Publications, 1977.

Nomenclature

$H_{12} = t + \left(\frac{H_1 + H_2}{2}\right)$	Distance between the centerlines of the glass layers
$I_1 = b\frac{H_1^3}{12}$	Moment of inertia of glass layer 1
$I_2 = b\frac{H_2^3}{12}$	Moment of inertia of glass layer 2
$I_T = I_1 + I_2 = b\frac{H_1^3 + H_2^3}{12}$	Moment of inertia of the glass layers
$Y = \frac{H_0^2 E_1 H_1 E_3 H_3}{E I_T (E_1 H_1 + E_3 H_3)}$	Geometric parameter

Appendix A

The Prony series for the shear relaxation modulus $G_t(t,T)$ is given by:

$$G_t(t) = G_0 \left\{ 1 - \sum_{i=1}^{n} g_i \left[1 - \exp\left(-\frac{t}{\tau_i} \right) \right] \right\} \tag{38}$$

where the parameters g_i and τ_i are shown in Table A1.

Table A1. Prony series coefficients for PVB.

Term	g_i	τ_i [s]
1	2.342151953E-01	2.36600000000000E-07
2	2.137793134E-01	2.26430000000000E-06
3	1.745500419E-01	2.16668000000000E-05
4	1.195345045E-01	2.07327300000000E-04
5	1.362133454E-01	1.98389580000000E-03
6	6.840656310E-02	1.89837195000000E-02
7	4.143944180E-02	1.81653498300000E-01
8	7.251952800E-03	1.73822593210000E+00
9	2.825459600E-03	1.66329270788000E+01
10	2.712854000E-04	1.59158978189400E+02
11	4.293523000E-04	1.52297789909670E+03
12	9.804730000E-05	1.45732380763177E+04
13	5.274937000E-04	1.39449999999999E+05